International Journal of GEOMATE, Oct. 2023, Vol. 25, Issue 110, pp.148-158
ISSN: 2186-2982 (P), 2186-2990 (O), Japan, DOI: https://doi.org/10.21660/2023.110.3941
Geotechnique, Construction Materials and Environment

STUDY OF A METHOD FOR EXTRACTING SMALL-SCALE TOPOGRAPHIC IRREGULARITIES USING WAVELET ANALYSIS MAPS

* Masafumi Imanishi[1], Koichi Nakamura[2] and Satoshi Nishiyama[3]

[1] WESCO Inc, Tottori, Japan, [2]Faculty of Engineering, Tottori University, Japan,
[3]Graduate School of Environmental and Life Science, Okayama University, Japan

*Corresponding Author, Received: 8 May 2023, Revised: 6 Aug. 2023, Accepted: 9 Aug. 2023

ABSTRACT: Microtopography and topographic parameter maps created from aerial laser profiler (LP) survey data are increasingly being used for business purposes. Wavelet analysis maps, unlike slope gradation maps, can be used to extract topographic irregularities without being affected by slope inclinations. First, a simulated terrain was created by changing the slope and the size of steps, and the size of steps that can be represented by a wavelet analysis map and by a slope gradation map was examined. Next, we examined the size of steps that can be extracted from the wavelet analysis and the slope gradation map for a slope with an average value of approximately 40 degrees, including the source of falling rocks, by using the results of the field survey. The size of the steps that can be extracted from the wavelet analysis map is approximately 2 m, and with the slope gradation map, it is more than 4 m. Hence, the wavelet analysis map is more accurate than the slope gradation map. Therefore, the wavelet analysis map can be used to extract smaller steps than those obtained with the slope gradation map.

Keywords: Wavelet analysis map, Aerial laser survey, Terrain interpretation, Microtopography

1. INTRODUCTION

In recent years, microtopography maps have become increasingly popular for business purposes. Because microtopography maps are created by superimposing various filters, a variety of methods have been proposed to create these maps by combining various approaches [1-8]. The microtopography map is created by transparently combining the numerical topographic data with the results of applying a filter that can represent changes in slope (slope gradation map [1] or vertical light source shading map [6]) and a filter that can extract the degree of unevenness of the terrain (ridge valley map[2], Curvature map [3], aperture map [4], wavelet analysis map [4, 5], multiple light source shading map [7]), or a elevation gradient map [8]. Microtopography maps are created using ground data acquired by navigational aerial laser profiler (LP) and drone LiDAR, which have a grid size smaller than that of GSI topographic maps and a 5-meter digital elevation model (DEM). The grid size is often 1.0 m or 0.5 m. The microtopography maps created in this way are used to extract landslide topography, small cliffs, and topographic irregularities, as well as to study rockfall sources [9-13]. The microtopography map is created by superimposing two maps of topographic quantities that are colored with coefficients obtained by filtering. One of them is a microtopography map created by superimposing a wavelet analysis map and a slope gradation map. The wavelet analysis map is created by coloring the wavelet coefficients.

The wavelet coefficients are characterized by the fact that their positive and negative values correspond to the uneven-ness of the terrain without being affected by the slope inclination angle.

The wavelet coefficients are not affected by the slope angle, and the wavelet coefficients correspond to the positive and negative values of the wavelet coefficients. For this reason, microtopographic maps are suitable for use at scales that do not show contour lines. In contrast, road disaster prevention inspections that require the resolution of relatively small geographic features such as exposed rocks, boulders, and small cliffs use road registers of approximately 1/500 scale. At this scale, large objects can be read from contour and slope gradation maps. However, the slope gradation map has the problem that it is difficult to distinguish between hue change due to slope inclination and hue change due to the geographic feature to be deciphered. In addition, since the microtopography map is created by superimposing a wavelet analysis map and a slope gradation map, it includes the aforementioned problems of the slope gradation map, and since the three primary colors make the hue darker and blacker due to the superimposition of images, it is more difficult to read geographic features from the hue changes than with the wavelet analysis map on its own. For this reason, previous studies on rockfall source extraction using support vector machines, one of the pattern classification methods, have used wavelet analysis maps instead of microtopographic representation maps that superimpose two topographic quantity maps. However, although there have been studies on the relative height differences that can be extracted from microtopographic maps that superimpose wavelet analysis and slope gradation maps, there have been no studies using only wavelet analysis maps. Therefore, it is necessary to study the relative height difference that can be read from the wavelet analysis map. The purpose of this study is to extract exposed rocks, boulders, and small cliffs. However, it is not possible to distinguish exposed rocks, boulders, and small cliffs from each other, although the points where differences in relative height exist an be identified from the microtopography and wavelet analysis maps. To distinguish between them, it is necessary to understand the planar extent and shape of the difference in specific elevation from the microtopography and wavelet analysis maps. By adding information from slope and contour maps to these maps, the survey should be conducted efficiently and without missing anything, and exposed rocks and boulders that may be the source of rockfall and landforms to be focused on should be identified.

In this study, we examined the differences in relative height that can be read from wavelet analysis maps using the results of field surveys. As a comparison, we also examined slope gradation maps used to create microtopographic representation maps. The ground data density in the study area was also examined be-cause the ground data density is important for representing smaller landforms. In this study, the grid size was set at 0.5 m.

2. RESEARCH SIGNIFICANCE

In this study, we investigated the readable difference in the relative height between the wavelet analysis map and the slope gradation map by using the results of a field survey of a slope where a source of falling rocks was located. It was found that the wavelet analysis map can decipher the relative height difference smaller than the slope gradation map. The wavelet analysis map is not affected by the slope inclination, unlike the slope gradation map. Therefore, it can be said that the wavelet analysis map is useful for extracting the source of falling rocks.

3. HOW TO CREATE A WAVELET ANALYSIS DIAGRAM

3.1 Calculation Method

Two-dimensional wavelet analysis can represent the degree of correlation between waves and undulations by continuously fitting a wave function called the "mother wavelet function" to the undulations of the terrains surface [4, 5, 14]. The analysis method uses Equation (1) to obtain the wavelet coefficients $C(s, a, b)$ is, which are obtained from the DEM using Equation (1) [15].

$$C(s,a,b) = \frac{1}{s}\iint z(x,y)\psi\left(\frac{x-a}{s},\frac{x-b}{s}\right)dxdy \qquad (1)$$

where a and b are the values of x and y values are the coordinates of arbitrary points in the DEM data. The $z(x, y)$ values are the DEM elevation values corresponding to the x, and y values are the DEM elevation values corresponding to the coordinates. Furthermore, the function of Eq. ψ is the mother wavelet, and the Mexican hat function shown in Equation (2) is used in this study.

$$\psi(x,y) = (2 - x^2 - y^2)e^{-0.5(x^2+y^2)} \qquad (2)$$

In this operation, the correlation between the Mexican hat function ψ and the ground surface shape is calculated from the convolution integral of equation (2), and the result is $C(s, a, b)$. Note that s is the scale factor of the Mexican hat function.

The Mexican hat function for a 1D shape is shown in Fig.1. The horizontal axis corresponds to the grid, and the vertical axis is the height of the Mexican hat function. The height of the Mexican hat function reaches its maximum at the center where the abscissa is zero, and the value decreases as the abscissa moves away from the center, taking a negative value and then reaching zero at the limit. In this case, the wavelength from the grid where the Mexican hat function reaches its maximum to the limit is expressed by the following equation using s [4].

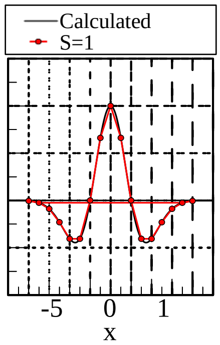

Fig.1 Mexican hat function

$$\lambda \fallingdotseq 4s \qquad (3)$$

Here, since the DEM is discretized data, the Mexican hat function must be discretized when the DEM is wavelet wavelet-transformed. In this study,

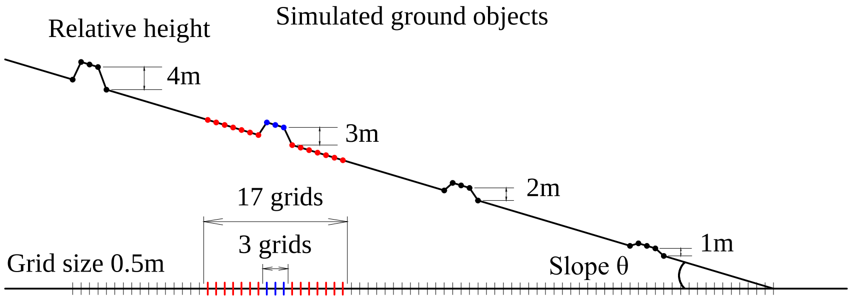

Fig.2 Simulated geotechnical model on a slope

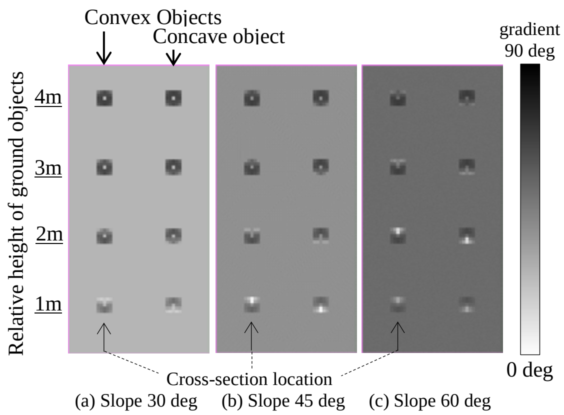

Fig.3 Slope gradation map of Simulated ground objects

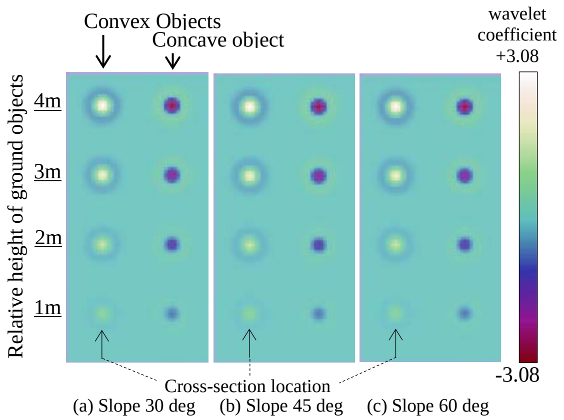

Fig.4 Wavelet Analysis map of Simulated ground objects

the grid size was set to 0.5 m and s = 1, which yields λ = 4. The discretized Mexican hat function is then represented by 17 grids of -4 to +4, as shown in the figure, and the wavelet coefficients are obtained as the product of the Mexican hat function.

3.2 Visible Representation Method

Topographic quantity maps are created by coloring the values calculated by some filter. For example, a slope gradation map is created by gradation using two colors corresponding to slopes varying from 0 to 90°. As mentioned above, the wavelet coefficient expresses the degree of correlation between the undulations of the land surface and the Mexican hat function. Therefore, the wavelet coefficient is positive for convex terrain, negative for concave terrain, and zero for flat terrain. Therefore, the wavelet analysis map should allow visualization convex, concave, and flat terrain by using a gradation of three or more colors corresponding to the positive, zero, and negative values of the wavelet coefficients. In this study, we used a gradation of white → green → light blue → violet → purple, corresponding to the convex, flat, and concave portions of the terrain, so that the terrain can be easily identified from the wavelet analysis map. White and green are positive values, light blue is zero, and violet and purple are negative values. The minimum and maximum value settings are problematic for the color scheme. For example, the wavelet coefficient may be locally large due to extreme topographic unevenness, man-made landforms, or man-made structures such as erosion control weirs. If the wavelet coefficients at such points are used as the minimum and maximum values, the undulations of the terrain cannot be adequately represented by gradation. In this study, wavelet coefficients are organized by percentiles, and wavelet analysis diagrams are created using the 5th percentile and 95th percentile values as the minimum and maximum values, respectively. The setting of the minimum and maximum values should be considered in the future since it affects the decipherment results using wavelet analysis diagrams.

4. STUDY USING SIMULATED TERRAIN

4.1 Simulated Terrain Model

The simulated terrain model was created based on the following ideas. The geometry of horizontal objects (number of grids) was set based on the concept of CCD (CCD image sensor) spatial resolution, which states that three pixels are necessary to faithfully reproduce an object [16]. Therefore, the size of the horizontal geographic

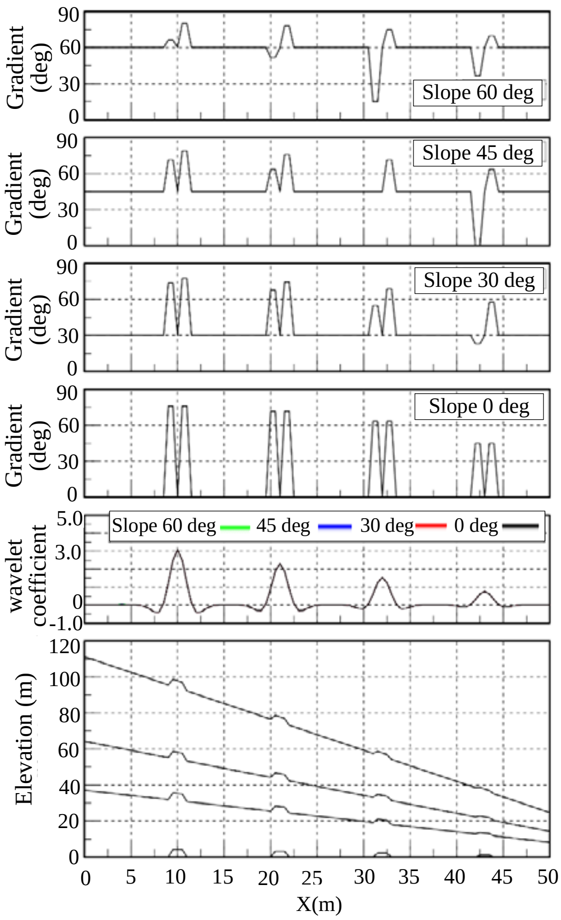

Fig.5 Correspondence between topography, wavelet coefficients, and slope

feature was represented by nine 3 x 3 (1.5 m x 1.5 m) grids. The number of vertical grids representing the relative height difference was set to 1 m, 2 m, 3 m, and 4 m, which are multiples of the grid size. The topography was created on slopes with slope angles of 30, 45, and 60 degrees. The tops of the landforms were set to the same slope angle. Fig.2 shows a cross-section of the simulated convex terrain, and the concave terrain is the inverted version of the convex terrain. Fig.2 shows the calculated range when the zero-horizontal axis of the Mexican hat function shown in Fig.1 is at the center of the top edge of the convex terrain.

4.2 Comparison of Wavelet Analysis Map and Tilt Volume Chart

The slope gradation map of the simulated terrain is shown in Fig.3, and the wavelet analysis is shown in Fig.4. The wavelet coefficients are positive for convex and negative for concave. The wavelet coefficients are colored from white to green, light blue, violet, and purple, corresponding to positive to negative values, in order to express the convexity and concavity in terms of hue. Fig.5 shows the correspondence between topography, wavelet coefficients, and slope, and Fig.3 and Fig.4 show the locations of the cross cross-sections compared. The slope gradation map was created using the method described in the reference.

Fig.5 shows that the wavelet coefficients are not affected by the slope angle, but vary with the relative height difference of the landform. The wavelet coefficients represent the unevenness of the terrain according to the size of the scale factor. For a grid size of 0.5 m and s = 1, Fig.5 shows that a Mexican hat function encompasses a 1.5m times 1.5m area. If the scale factor is further reduced, a single landform is represented by multiple Mexican hat functions, and the hue change becomes more complex and difficult to distinguish. Therefore, it is necessary to select an appropriate scale factor according to the size of the geographic feature or landform to be represented by hue.

Fig.5 shows that the amount of slope varies according to the relationship between the slope angle and the relative height difference of the landforms. Fig.5 shows that the larger the slope angle is, the smaller the change in the amount of slope due to geological features, making it difficult to discriminate the slope by through hue change. In addition, depending on the relationship between the slope angle and the relative height difference between the landform and the slope angle, the slope angle may be smaller than the amount of slope amount of the slope.

Thus, wavelet analysis maps can show changes in the relative height difference of landforms without being affected by the slope gradient. However, unlike slope gradation map, wavelet analysis maps cannot represent slope inclination, and must be used in combination with other charts, such as contour and slope gradation map.

5. STUDY ON THE SIZE OF STEPS THAT CAN BE EXTRACTED USING THE RESULTS OF THE FIELD SURVEY

5.1 Slope and Ground Data Density Under Consideration

Fig.6 shows an orthophoto of the slope under study. In this study, we used ground data measured in winter along Route 53 in Okayama Prefecture, Japan. The ground data were measured in winter to improve the ground data density [9].

Ground data density greatly affects how well the grid data represent the terrain. The point cloud density is 6.5 points/m^2, but the actual ground data distribution is sparse, so an evaluation of the distribution was conducted. The purpose of this

Fig.6 Orthophotograph of the study area

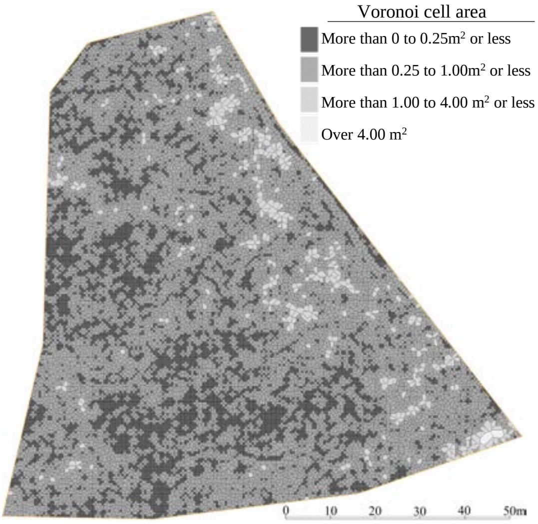

(a) 0.5m grid

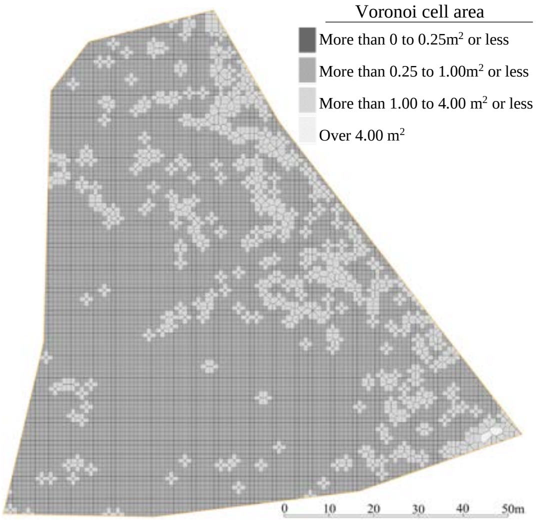

(b) 1.0m grid

Fig.7 Voronoi partition diagram considering the distribution of ground data

study is to extract the unevenness of the terrain. When ground data do not exist for a grid with uneven terrain, the grid without ground data is created by interpolation from the surrounding ground data. This results in a smaller or smoother local slope angle at the steps, making it difficult to extract the unevenness of the terrain. Therefore, it is important to understand the distribution of ground data.

There are two methods for evaluating ground data other than point cloud density. One is to use triangular irregular networks (TINs) created from ground data to obtain the maximum edge length from all TINs containing the ground data to be focused on and to use this as information to evaluate the points of interest [17]. When the grid size is 0.5 m, the edge length of the TIN is 0.5 m or approximately 0.71 m for ideal ground data. If the edge length differs from this, it can be said that there are many distorted TINs. The other method is to divide the TIN into Voronoi cells and evaluate the ground data by giving the area of the Voronoi cell or the reciprocal of the area as information [18]. When the grid size is 0.5 m, if the area of the Voronoi cell is larger than 0.25 m^2, the distribution of the ground data is biased. From this, it is easy to understand the distribution status of the grid created by interpolation.

In this study, the Voronoi partitioning method was used for evaluation, and the process was as follows. The number of ground data points was given to the grid center coordinates, the center coordinates with no ground data were deleted, and the remaining center coordinates were used for Voronoi segmentation. If all grids have ground data, the Voronoi segmentation result is the same as that of the grid. Fig.7 shows the results for grid sizes of 1.0 m and 0.5 m. For a grid size of 1.0 m, approximately 95% of the Voronoi cell area is less than 1 m^2. However, for a grid size of 0.5 m, approximately 95% of the Voronoi cell area is less than 1 m^2.

However, for a grid size of 0.5 m, approximately 45% of the Voronoi cell area corresponds to 0.25 m^2 or less. Although a grid size of 0.5 m is considered in this study, the distribution of ground data is shown in Fig.7, and it is considered that the relative height difference that can be extracted differs de-pending on the location.

In recent years, contour and slope gradation maps have often been created from 1.0 m or 0.5 m grids generated from navigational LPs. This makes it possible to decipher topographic changes that are smaller than the GSI's 5-meter DEM. Fig.8 shows the slope gradation map, and Fig.9 shows the wavelet analysis map. One-meter contours created from the grid data are also superimposed on each figure.

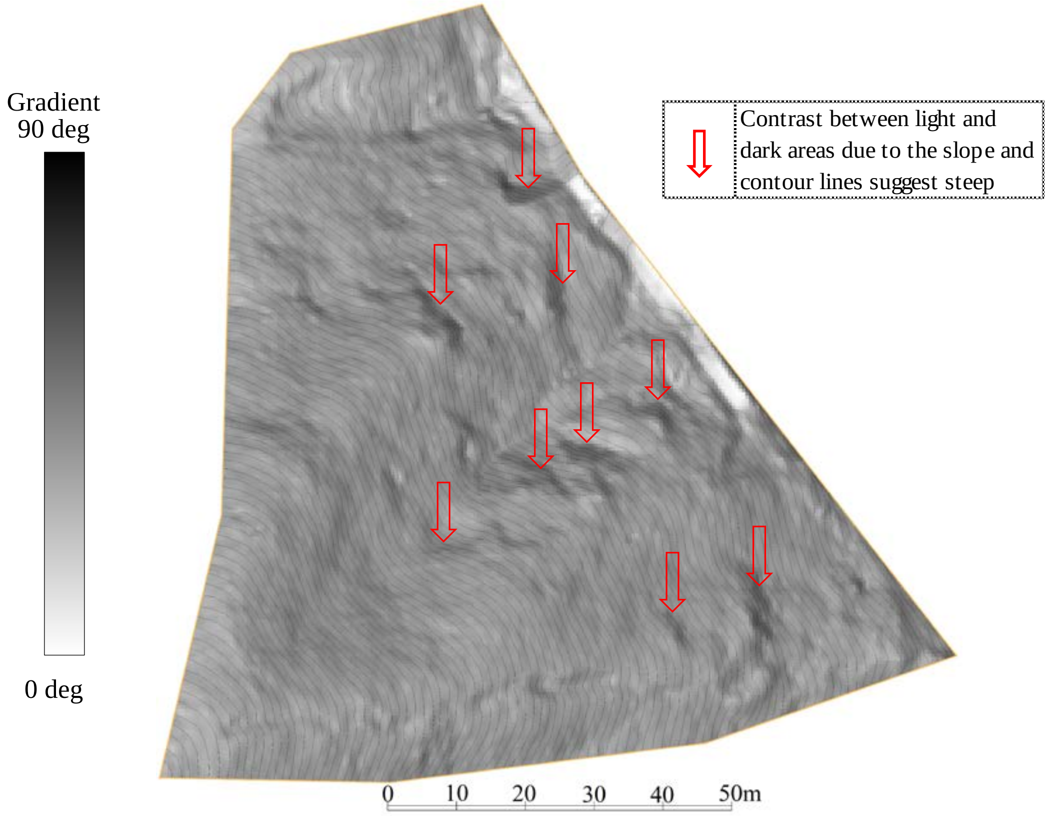

Fig.8 Slope gradation map

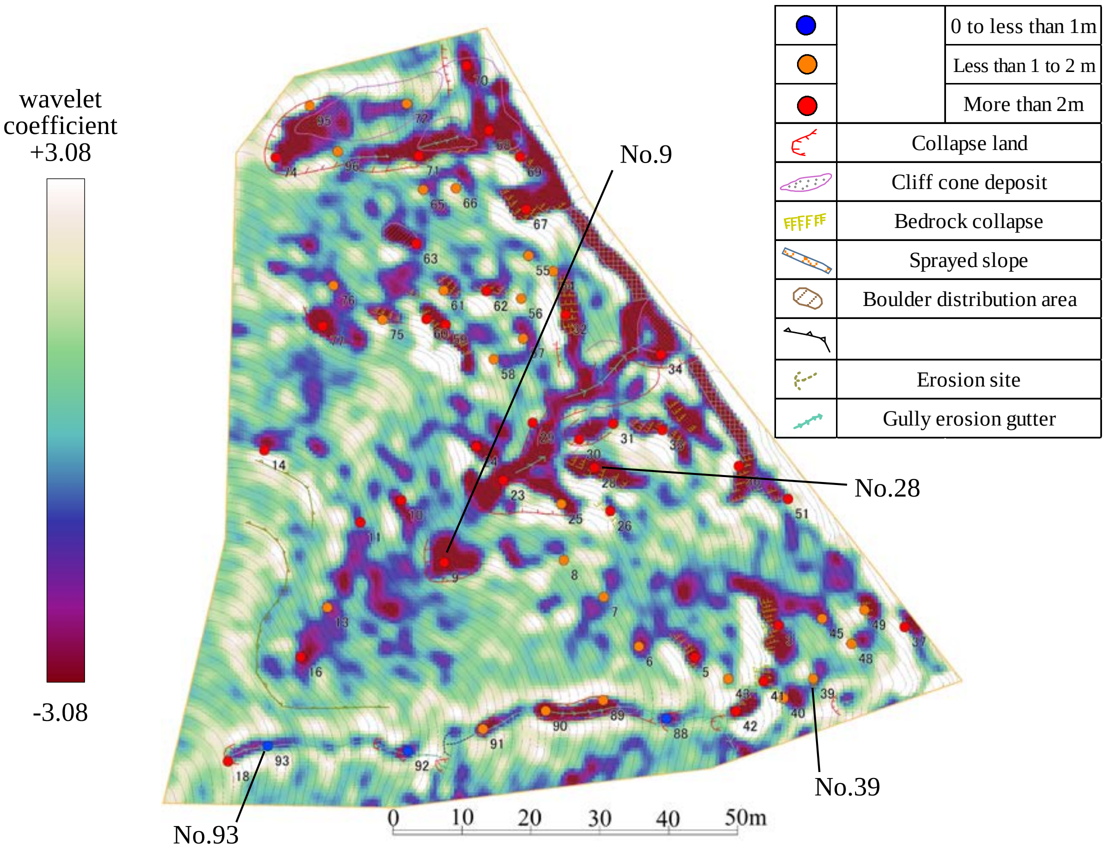

Fig.9 Wavelet analysis map and field survey results

5.2 Examination of the Size of Steps that can be Extracted from The Slope Gradation Map and Wavelet Analysis Maps using The Results of The Field Survey

The points of interest were identified by linking the wavelet analysis map stored in a tablet PC brought to the site with the GPS function. Because of the poor reception of signals from GPS satellites in mountainous forests, the results of independent positioning drifted randomly by approximately 10 meters. The location of the target points was determined by taking into account the results of the engineer's visual inspection of the site.

The survey results indicate that the slope is a bedrock slope formed from Paleozoic slate and sandstone with thin topsoil and that there are many terrain features, such as exposed rocks, boulders, collapsed sites, and ditch-like erosion sites. Sixty-four topographic features were found on the slope with an average slope of more than 40 degrees. The breakdown of the terrain irregularities, classified by relative height difference, was as follows: 34 were greater than 2 m, 27 were greater than 1 m and less than 2 m, and 3 were less than 1 m. The average slope was more than 40 degrees (Fig.9).

The contrast of the slopes with partial slopes of 60° is noticeably darker than the surrounding areas, and the contour interval is 4 to 5 m. This suggests the presence of significant topographic irregularities, such as cliff faces. The slope gradation map shows nine locations (Fig.8).

In the next section, the magnitude of the steps that can be extracted is discussed by comparing the wavelet analysis map and the slope gradation map in which the treading results are filled in.

a) Comparison at locations with a step difference of 4 m or more

Consideration will be given to point No. 28. From the survey, it was confirmed that the ridge is a convex ridge with a bedrock outcrop and that the difference in relative height between the foot and head of the outcrop is approximately 5 m (Fig.10a). The slope contrast between the topography of the ridge and the topography of No. 28 is shown in Fig.10b. The contrast between the light and dark areas on the slope gradation map indicates that the topography is uneven. In the wavelet analysis, a clear hue change from "white to red" is distributed along the contour line, corresponding to the convex topography from the head to the shoulder of the exposed rock and the concave topography flowing from just below the cliff to the foot. The area highlighted in "white" corresponds to the convex shape of the exposed rocks, and the area highlighted in "red" corresponds to the location where the slope changes to a gentle slope in the de-pression just below the cliff. The "white to red" boundary appears between the points where the slope changes (Fig.10c).

Consideration will be given to point No. 9. From the inspection, the slope above the cliff was relatively uneven, and then it changed to a steep slope of approximately 45 to 60 degrees with a relative height difference of approximately 4 m (Fig.11a). The slope contrast shows the existence of a head cliff. The dark contrast in the slope profiles indicates the presence of a head slope (Fig.11b). In the wavelet analysis, the hue change from "blue to red" corresponds to the transition from a smooth slope above the cliff to a pronounced concave topography, and the red horseshoe-shaped area corresponding to a moving soil mass is clearly visible in plain sight. The area highlighted in "blue" corresponds to the convex shape of the cliff shoulder, and the area highlighted in "red" corresponds to the horseshoe-shaped concave depression. The "blue to red" boundary appears around the midpoint of the cliff between the slope change points (Fig.11c).

The above results suggest that topographic irregularities with a relative height difference of 4 m or more can be extracted from both the slope gradation map and wavelet analysis maps. The Voronoi partitioning diagrams for both No. 28 and No. 9 show that some grids near the focus point were created by interpolation (Fig.10d, Fig.11d). The Voronoi cell area ranges from more than 0.25 to less than 1.00 m^2, which is equivalent to a grid size of 1 m. Therefore, a ground data density equivalent to a grid size of 1 m is not expected to affect the extraction of topographic irregularities with a relative height difference of 4 m or more.

b) Comparison at locations with less than 2 m of steps

Consideration will be given to point No. 39. From the field survey, we observed a concave topography formed by a small drop formed by a rock mass exposed at the edge of a relatively smooth slope and its base. The outcrops and other localized areas have a drop of approximately 1.5 m (Fig.12a). The slope gradation map shows that the outcrops are located in a relatively smooth slope (Fig.12b). The contrast between light and dark areas on the slope gradation map is not clear, so it is difficult to determine the topography as uneven. In the wavelet analysis map, a small "green to blue" hue area coincides with the survey point (Fig.12c). This corresponds to the hue change of the concave topography shown in the simulated terrain.

Consideration will be given to point No. 93. From the inspection, the difference in specific elevation between the center of the small ditch-like depression and the shoulder of the sidewall is approximately 0.6 m. However, including the mound-like bulge on the periphery of the depression, the difference in specific elevation is approximately 1 m (Fig.13a).

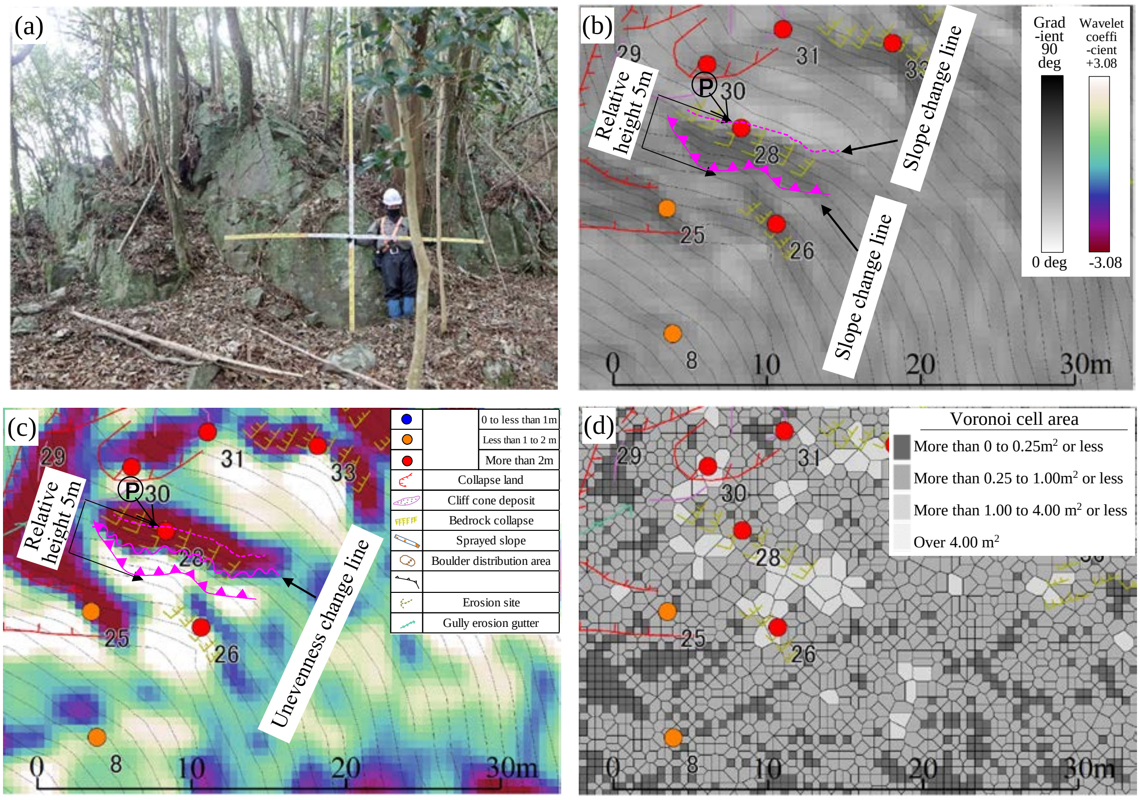

Fig.10 Photographs, Slope gradation map, Wavelet analysis map and Voronoi partition diagram for location No. 28

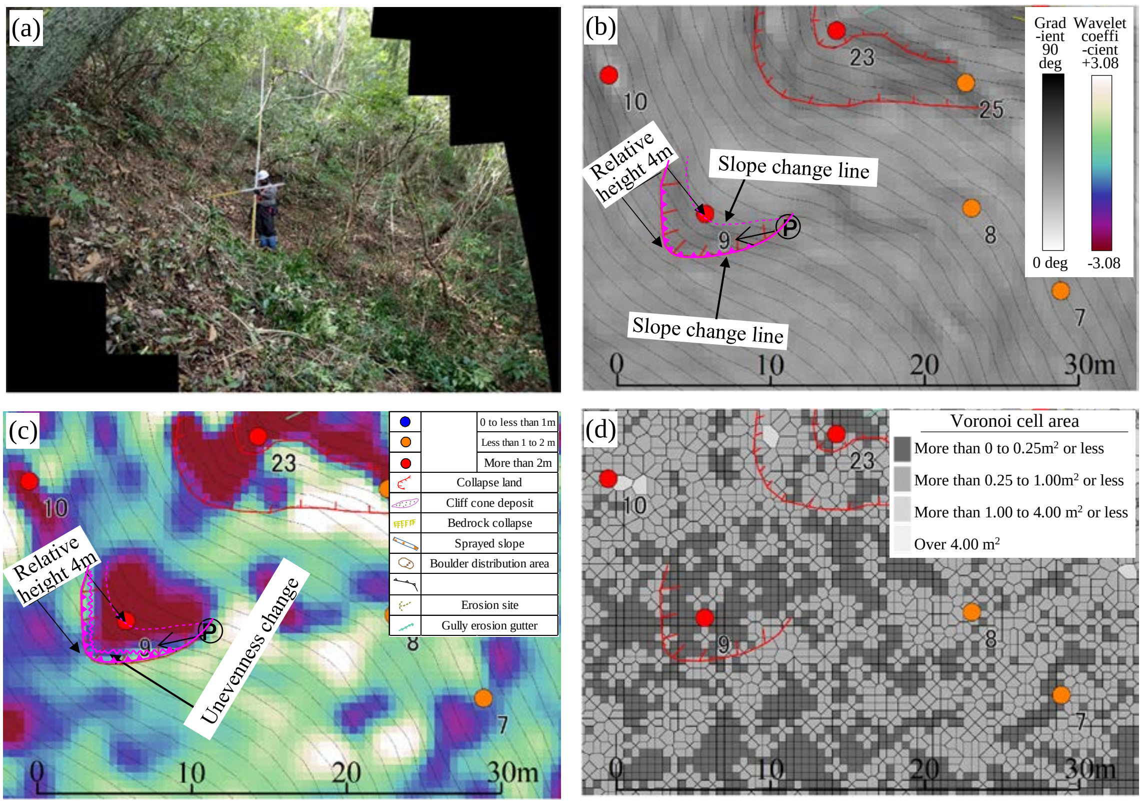

Fig.11 Photographs, Slope gradation map, Wavelet analysis map and Voronoi partition diagram for location No. 9

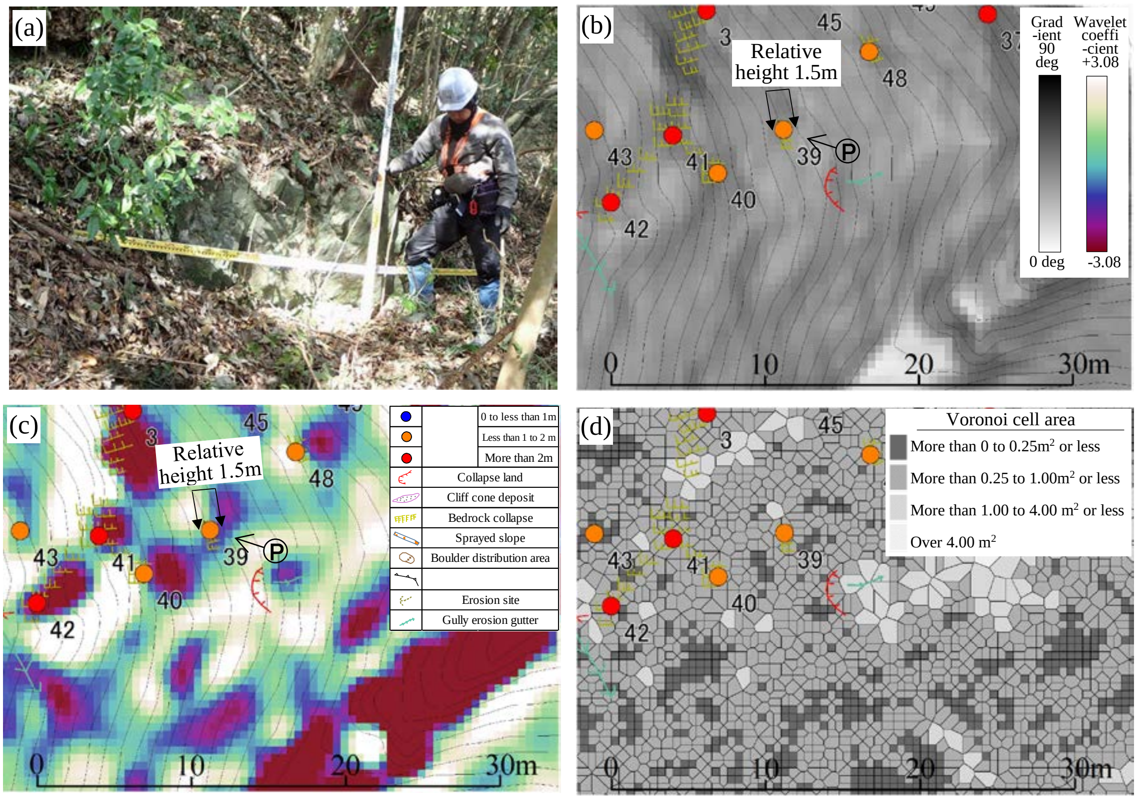

Fig.12 Photographs, Slope gradation map, Wavelet analysis map and Voronoi partition diagram for location No. 39

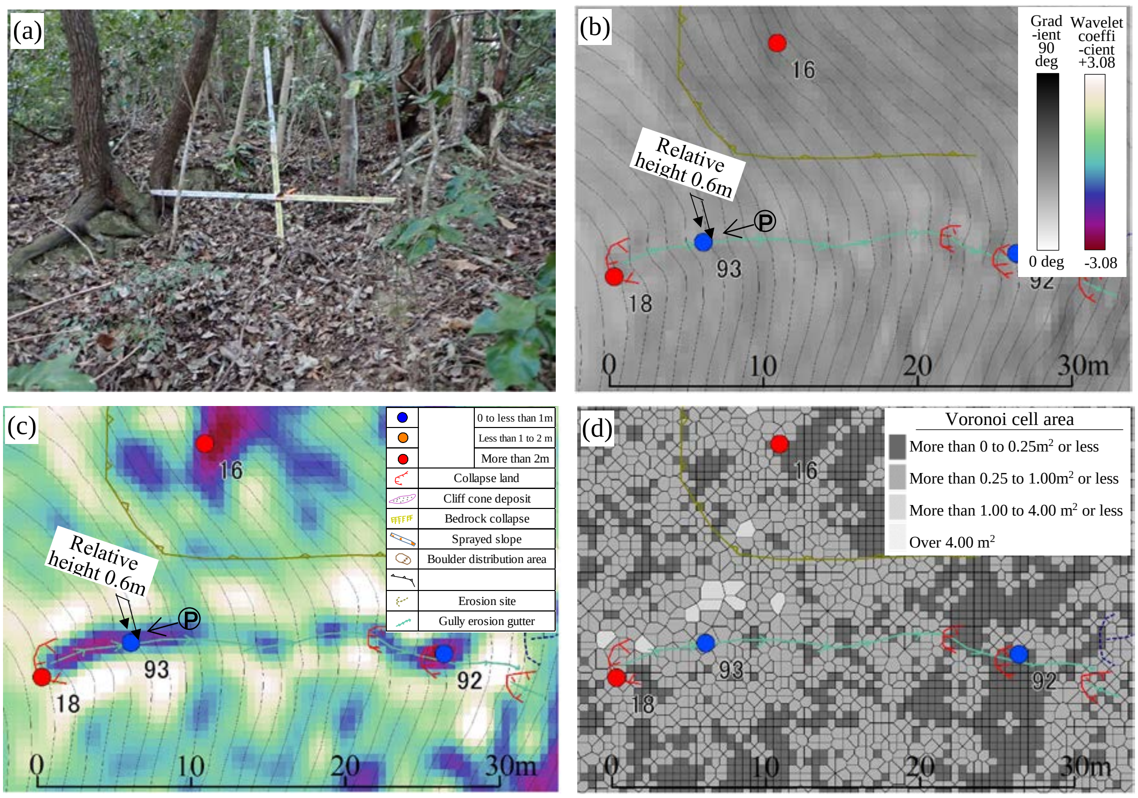

Fig.13 Photographs, Slope gradation map, Wavelet analysis map and Voronoi partition diagram for location No. 93

Microtopography with continuity, such as ditch topography, gully erosion sites, and road networks, is considered to be easy to extract even if the difference in specific elevation is smaller than 1 m.

From the above, it can be said that it is difficult to extract the unevenness of landforms with a relative height difference of less than 2 m from the contrast between bright and dark areas in the slope gradation map. On the other hand, the wavelet analysis map can well extract convex and upward-peaking topographic features such as exposed rocks and steep cliffs, which are represented by the "red to white" hue change, and the gentle "green to blue" hue change can extract small-scale exposed rocks that are exposed at the edge of relatively smooth slopes. The "green to blue" hue change may also correspond to the presence of unevenness in small, exposed rocks at the edge of relatively smooth slopes or in concave landforms such as shallow gouge-shaped landforms. The Voronoi partitioning diagram shows that the grids around the focus points in both No. 39 and No. 93 were created by interpolation (Fig.12d, Fig.13d). The Voronoi cell area ranges from more than 0.25 to less than 1.00 m^2, which is equivalent to a grid size of 1 m, similar to No. 28 and No. 9. The wavelet analysis map is considered to be more suitable than the slope gradation map for the extraction of topographic irregularities with a relative height difference of less than 2 m.

6. CONCLUSION

The results of this study are summarized below.

1) By comparing the wavelet analysis map with the survey results, we were able to extract all convex and concave landforms with a relative height difference of 2 m or more. The hue is expressed as a change from "white to red" for convex terrain and "green to red" for concave terrain.

2) The wavelet analysis map was compared with the survey results, and it was found that even with a relative height difference of 1 m or less, there is a possibility of extracting a continuous ditch-like concave topography, although it is affected by the distribution of ground data and other factors. The color hue was similar to that of a relative height difference of 1 m or more, or "green to blue" in some cases.

3) The slope gradation map also uses contour lines so that topographic irregularities with a relative height difference of 4 m or more can be extracted.

Previous studies using microtopographic maps created by superimposing wavelet analysis and slope gradation maps have reported that topographic features with a relative height difference of 2 m or more can be extracted.

This study shows that the wavelet analysis map can extract specific elevation differences of 2 m or more, similar to previous studies. However, for a continuous ditch-like concave topography, it is possible to extract from a relative height difference of 1 m, which is smaller than that of a microtopographic map. This study was conducted using a slope with an average angle of 40°, and it can be said that a wavelet analysis map is more suitable than a slope gradation map for extracting small topographic relief on a steeper slope.

7. REFERENCES

[1] Kamiya, I., Kuroki, T. and Tanaka, K., Interpretation of geomorphology and geology using slope gradation map, Geoinformatics, Vol.11, No.1, 2000, pp. 11-24.

[2] Chiba, T. and Suzuki, Y., `Red Relief Image Map`- The new visualization method, Journal of Applied Survey Technology, Vol.15, 2004, pp. 81-89.

[3] Toda, K., Development of the microtopographical map by using airborne LIDAR DEM, JSECE Journal, Vol.65, No.2, 2012, pp. 51-55.

[4] Fujisawa, K. and Kasai, M., Manual of analysis of areal laser survey data in landslides (Draft), Technical note of PWRI, No.4150, 2009.

[5] Asahita, T., Microtopography extraction by wavelet transform, Microtopography extraction by wavelet transform, 2014, pp. 7-8.

[6] Akiyama, Y. and Sekoguchi, R., IN-YOU-ZU diagram with excellent microtopographic representation, Map, 45, No.1, 2007, pp. 37-46.

[7] Suzuki, K. and Ishikawa, G., Research related to terrain representation by multiple light source shading and oblique illumination method pseudo-shading, Association of Precise Survey & Applied Technology, Vol.109, 2017, pp. 34-41.

[8] Sasaki, H. and Mukoyama, S., ELSAMAP (Elevation and slope Angle Map) with airborne laser scanner DEM, Journal of the Japan Society of Engineering Geology, Vol.49, No.6, 2009, pp. 318-330.

[9] Miyashita, M., Imanishi, M., Miyata, M. and Nishiyama, S., Verification of specification method of falling rock generation source using highlighting map of microgeomorphology created by high density aerial laser data, Journal of Japan Society of Civil Engineers, Ser. F3 (Civil Engineering Informatics), Vol.73, No.2, 2017, pp. I_92-I_108.

[10] Kikuchi, T., Hatano, T., Senda, Y. and Nishiyama, S., Development of analytic method for landslide measurement by movement vectors using S-DEM data obtained from airborne laser point clouds, Journal of the Japan Society of Engineering Geology, Vol.57, No.6, 2017, pp. 277-288.

[11] Miura, K. Komuro, H. and Kuramoto, N., Extraction of rock-fall danger points related to road disaster prevention using laser profiler data, Journal of JGS, Vol.69, No.6, 2021, pp. 30-33.

[12] Sakita, K., Kikuchi, T. and Nishiyama, S., Identification of rockfall source based on terrain analysis map using support vector machine, Japanese Geotechnical Journal, Vol.17, No.2, 2022, pp. 147-157.

[13] Sakita, K., Kikuchi, T. and Nishiyama, S., Source extraction of rockfall by microtopography highlight map via high-density aerial laser survey, International Journal of GEOMATE, Vol.22, No.94, 2022, pp. 1-12.

[14] Booth, A.M., Roering, J.J. and Perron, J.T., Automated landslide mapping using spectral analysis and high-resolution topographic data : Puget Sound lowlands, Washington, and Portland Hills, Oregon, Geomorphology, Vol.109, No.3, 2009, pp. 132-147.

[15] Paul, S. A., The illustrated wavelet transform handbook, CRC Press, 2016, pp. 464.

[16] James B. Pawley, Points, pixels, and gray levels, Digitizing image data, Handbook Of Biological Confocal Microscopy, Springer, 2006, pp. 59-79.

[17] Naus, M.T., Lidar Density and Spacing Specification Version 1.0. Retrieved July 23, 2017, http://www.asprs.org/wp-content/up-loads/2010/12/Naus.pdf.

[18] KODORS, S., Point Distribution as True Quality of LiDAR Point Cloud, Baltic J. Modern Computing, Vol.5, No.4, 2017, pp. 362-378.

Copyright © Int. J. of GEOMATE All rights reserved, including making copies, unless permission is obtained from the copyright proprietors.